The International Journal of Advanced Manufacturing Technology (2019) 102:1497–1507
https://doi.org/10.1007/s00170-018-03259-9

ORIGINAL ARTICLE

An artificial neural network model for laser transmission welding of biodegradable polyethylene terephthalate/polyethylene vinyl acetate (PET/PEVA) blends

Mehrshad Mehrpouya[1] · Annamaria Gisario[2] · Atabak Rahimzadeh[2] · Massimiliano Barletta[1]

Received: 25 September 2018 / Accepted: 26 December 2018 / Published online: 8 January 2019

Abstract
Laser transmission welding is a quick, easy, and viable method to join plastic materials for several industrial domains. The main challenge for manufacturers is still on how to choose the input process parameters to achieve the best joint performance. Joining between PET (polyethylene terephthalate) films does not make an exception, with quality strictly depending on laser joining parameters. The purpose of the present study is to estimate the weldability of a polymeric material couple according to their thermal and optical properties. This paper investigates an experimental study of laser transmission welding of PET 100% and PET-PEVA (polyethylene vinyl acetate) 5%, 10%, and 15% sheets by a diode laser. In the present work, laser power and scan speed were considered as operational parameters, which have a significant influence on the quality of the joint zone. Then, the influence of PEVA aliquots in PET/PEVA blends, which altered the mechanical properties, such as joining behavior, mechanical characterization, and degradation level, was analyzed. In addition, an artificial neural network model is developed to achieve the optimal laser parameters. The obtained results proved the advantage of this model, as a prediction tool, for developing laser welding parameters.

Keywords Laser transmission welding · Biodegradable polymer · Poly(ethylene terephthalate) · PET · Artificial neural network

1 Introduction

Plastic materials can be applied in small-scale components such as medical and electronic devices, food containers, sensor enclosures, or consequently in the manufacturing of components for large-scale projects such as automotive, aerospace, and construction industries. Being an attractive developing field, researchers are looking for some new methods to optimize the manufacturing processes such as joining techniques [1, 2]. One of the most applicable plastic materials is poly(ethylene terephthalate) which is widely used in the shape of foils and sheets in various manufacturing processes and products. This polymer, which commercially is well known as PET, can be used for a wide range of products from food to drug packaging items because of its good thermal stability, impermeability, and dielectric properties [3]. The application of biodegradable polymers has attracted many attentions due to their reduced environmental impact. The possibility to develop simple processing of biodegradable plastic can increase their potential, as they could be processed at a high rate with a reasonable cost. Accordingly, the joining of these biodegradable polymers can make a great opportunity to be used in various products as well as their current applications in medical and electronic devices and sports equipment.

Laser transmission welding (LTW) is an appropriate and fast method for joining of thermoplastic components with durable and strong bond [4, 5]. This process is applied in welding of plastic materials in the packaging industry with a high quality and productivity, which highly depends on thermal parameters, light absorption, and light scattering [6]. In fact, these parameters can be utilized as a functional tool for optimization of the laser welding process [7–9]. Numerical computations can also simulate the welding process in order to achieve the optimized welding parameters and a prediction of material weldability [10–13].

✉ Mehrshad Mehrpouya
mehrshad.mehrpouya@uniroma1.it

[1] Dipartimento di Ingegneria, Università degli Studi Roma Tre, Via Vito Volterra 62, 00146 Rome, Italy

[2] Dipartimento di Ingegneria Meccanica ed Aerospaziali, Sapienza Università degli Studi di Roma, Via Eudossiana 18, 00184 Rome, Italy

Brown et al. firstly presented a laser transmission welding of multi-layer polymer for the manufacture of the food container. They applied opaque Nylon 66 as outer polymeric layer lids to a tubular container. The results demonstrated appropriate weld strength in the welded zone [4]. Ilie et al. investigated the weldability of PMMA (poly-methyl-meth-acrylate) and ABS (acrylonitrile-butadiene-styrene) by a combination of the both experimental and simulation methods. They used a thermal model to estimate the evolution of the temperature field and laser beam behavior at the interface of two components. They consequently proved the obtained results of the simulation with experimental results. This approach, as an efficient tool, determined the weldability of polymeric materials with a significant reduction in costs and time [14, 15]. Ussing et al. represented the micro-laser transmission welding of PETG (polyethylene-terephthalate-glycol) and Topas COC (cyclic-olefin-copolymer) by using a low power diode laser. They employed a wide range of parameters to achieve various targets such as welding width, speed, or precision. They alternatively treated the surface of PETG with IR absorber dye by applying a slender laser wavelength and the surface of Topas was coated by a thin layer of black carbon (5–10 μm) [16].

Spekta et al. also used the same IR thermography as a non-contact method for the laser transmission welding of ABS and PMMA polymeric materials. The results of the numerical modeling are compared with experimental temperature during heating and cooling of the process and the optimal process parameters ultimately are acquired by good matching between experimental and simulation [1]. Amanat et al. assessed the effect of laser parameters such as scan speed, laser power, and material morphology on weldability of PEEK (poly-ether-ether-ketone). They investigated the quality of the joint for semi-crystalline and amorphous PEEK materials and they found the higher bond strength for semi-crystalline materials compared to the amorphous polymer when the scan speed is the lowest [17]. Zak et al. investigated a laser transmission welding of PA6 (polyamide 6) and PA6GF (glass fiber reinforced polyamide 6) by a diode laser in order to explore the influence of laser power on weld line width. They employed a simple technique for the measurement of the energy distribution of a weld line without the application of sophisticated measurement equipment [2]. Chen et al. also described the effect of the absorption coefficient to measure the laser energy distribution as a function of part thickness for unreinforced PA6 and PA6GF as well as amorphous polycarbonate (PC) with or without carbon black (CB). This linear model made a relation between the amount of applied BC and the absorption coefficient in polymers based on the obtained experimental result of PA6, PA6GF, and PC [18].

Artificial neural network (ANN) is a powerful tool for the modeling of the relationships between variables which can learn and predict based on the experimental data. ANNs is recently applicable to various fields such as manufacturing and material processes. For example, Sterjovski et al. successfully applied an ANN model for predicting the mechanical properties of the welding steel materials [19]. Li-Ming et al. developed a neural network model for diffusion welding of SiCw/6061Al metal matrix composites and the predicted outputs had a good agreement with the experimental data [20]. Jeng et al. applied a back-propagation (BP) learning model for the prediction of laser welding parameters of a butt joint [21]. Acherjee et al. reported an artificial neural network model for laser welding of thermoplastic sheets that can successfully predict the relationship between the laser parameters (including laser power, scan speed, stand-off-distance, and clamp pressure) and joint quality (inducing strength and dimension of the joints) [22]. Wang et al. also applied an artificial neural network model for laser transmission welding of thermoplastic-polycarbonate (PC). Their model can predict the optimum laser parameters and the joint quality that the predicted values match well with the actual values [23]. In this respect, the present work deals with similar and dissimilar laser welding of PET and PET/PEVA polymer sheets by a diode laser. The purpose of the present study is to estimate the weldability of a polymeric material couple according to their thermal and optical properties. The laser joining was performed under a wide range of welding conditions. Then, joining behavior, mechanical characterization, and degradation level were analyzed in detail and the effectiveness of the process was discussed. Moreover, a correlation between the applied laser parameters and the achieved output was developed through a nonlinear model by applying ANNs. This model can be employed as a prediction tool to estimate the optimum weld based on various laser parameters including laser power and scan speed. The predicted achievements show a good agreement with the experimental data set.

2 Experimental setup

2.1 Material and equipment

In this study, Neopet 84 Poly(Ethylene Terephthalate) produced by Neogroup (UAB Neo Group, Rimkai, Lithuania) was investigated. This type of polymer is employed in various applications, mostly in packaging. This PET has a high intrinsic viscosity (0.84 ± 0.02 dL/g) and a melting temperature of around 250 °C. This PET can also be reprocessed and mixed with the other material by melt processing. Therefore, Neopet 84 was blended with PEVA (polyethylene vinyl acetate), a biodegradable polymer, with a melting temperature of around 105 °C. Consequently, four types of blends were produced for this investigation: PET 100%, PET-PEVA blends with 5, 10, and 15 wt% PEVA (i.e., the additive). All of the polymeric specimens have the same dimension with the length of 120 mm, the width of 28 mm, and thickness of 0.33 mm.

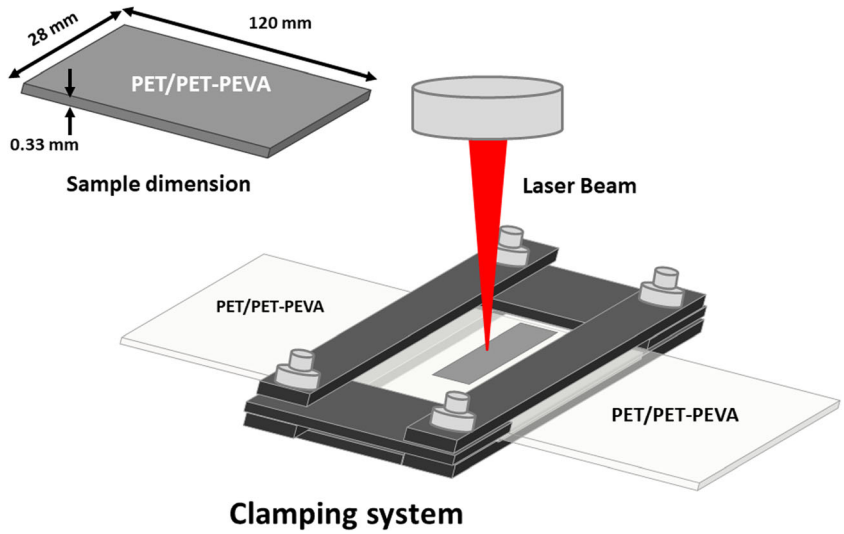

Fig. 1 The schematic of the clamping system and laser position

A high-power diode laser with a continuous wave (HPDL-CW, ROFIN-SINAR DL 015, Plymouth, Michigan) is employed in this experimental process. The laser equipment has a maximum power of 1500 W with a wavelength of 940 ± 10 nm. Also, the beam shape is elliptical with 1.2 mm × 3.8 mm axes. The shorter axis is parallel to the orientation of the laser scan. The focal distance of the lens, which was used during the experimental tests, is 63 mm, while the working distance is 32 mm. Argon gas (less than 1 bar) is also flushed to the melting zone during the process for protection and insulation purposes.

The mechanical response of the welded samples was investigated by a static testing machine (MTS Insight 5, MTS, Eden Praire, USA). All tests were implemented setting the deformation speed at 2 mm/min. This machine was connected to a computer system by a direct remote control and was calculated some parameters such as elasticity modulus, yield stress, breaking load, and elongation percentage.

2.2 Research method

All the samples were cleaned by a mix of detergent and water, then alcohol at the beginning to remove any contamination from the surfaces of the sheets. Then, as shown in Fig. 1, the overlapping samples were positioned in a simple clamping system, fixed by a screw and bolt system. After that, the laser parameters were set and the clamping system was positioned under the laser beam. The underlying surfaces were painted with a thin layer of black acrylate to improve the absorption of radiation during the laser transition welding. In fact, the heat absorption raises the local temperature and changes the polymer status, thus promoting the formation of the laser joints. The experiment was performed on PET 100% and PET-PEVA 5%, 10%, and 15% according to the operational parameters summarized in Table 1. As indicated, the tests included five different values of laser powers and three scan speeds, which applied for all polymeric samples. The experiment was operated with two replications to demonstrate reliability and repeatability of the experimental results.

3 Neural network solution

3.1 Neural network scheme

In this study, a set of two different neural network models is investigated to find the desirable solutions for predicting the experimental trends in similar laser welding of PET and PET-PEVA sheets based on all operational parameters:

- Generalized feed-forward (GFF-MLP) neural network
- Radial basis function (RBF) neural network

The algorithm of BP was used to train both of the (GFF-MLP) and (RBF) neural networks. The software simulator used was NeuroSolutions version 7.0.1.0 developed by NeuroDimension Incorporated.

Table 1 Setting of laser operational parameters

Type of polymers	PET 100%	PET-PEVA 5%	PET-PEVA 10%	PET-PEVA 15%	
Laser power (W)	50	60	70	80	90
Scan speed (mm/s)	6	8	10		

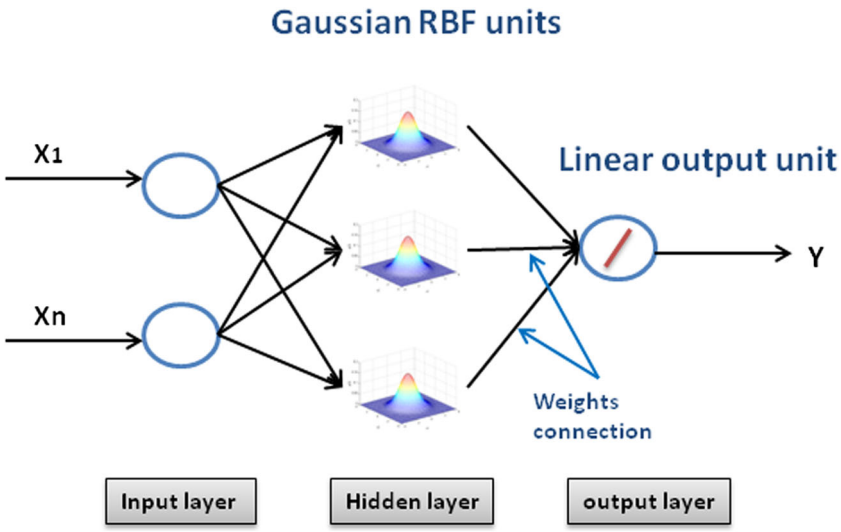

Fig. 2 A schematic of the RBF neural network and the relation of various layers

3.1.1 GFF-MLP

GFF-MLP is one of the most common artificial neural networks that applied for the connection between units without cycle form, since the information only travels forward in the network (no loops) [24, 25]. In fact, this model works based on the connection between input and output nodes (also hidden nodes if present) and there are no feedback connections in which outputs of the model are feedback into itself. Overall, GFF-MLPs neural networks are primarily used for supervised learning in cases where the data to be learned is neither sequential nor time-dependent [26].

3.1.2 RBF

Broomhead et al. introduced RBF networks as a class of ANN that can be used in many classification problems in science and engineering [27]. Rather than of having threshold units, each RBF neuron has a set of values named a "reference vector" for comparison with an input set of the same cardinality. The driving equation of individual neuron used in this study is based on the multivariate Gaussian function:

$$\varphi(r) = e^{\left(-\frac{1}{2\sigma_j^2}\|x-t_j\|^2\right)}$$

where x is the input vector for the neuron, t_j is the set of reference values, σ_j is the standard deviation (σ^2 is the variance) of the function for each of the centers (j), and the value r ($\|x-t_j\|$) is the Euclidean distance between a center vector and the set of data points [28]. Figure 2 shows a schematic of the RBF neural network that an input vector (X_1, X_n) was used as input to all radial basis functions for different parameters. The output of the network is a linear combination of the outputs from radial basis functions.

3.1.3 Back-propagation algorithm

In 1986, Rumelhart et al. proposed a systematic neural network training approach [29]. One of the significant contributions of their work is the error BP algorithm [30]. The main objective of this neural model is to find an optimal set of weight parameters (w), as a variant in the function of $y = y\ (x, w)$, which closely represents the original problem behavior. This is achieved through a process called training (that is, optimization in w-space). A set of training data is present to the neural network. The training data are pairs of (x_k, d_k), $k = 1, 2 \ldots p$, where d_k is the desired output of the neural model for inputs x_k, and p is the total number of training samples. During training, the neural network performance is evaluated by computing the difference between actual network outputs and desired outputs for all the training samples. The difference, also known as the error, is calculated by

$$E = \frac{1}{2}\sum_{k\in T_r}\sum_{j=1}^{m}\left(y_j(x_k, w) - d_{jk}\right)^2$$

where $y_j(x_k, w)$ is the jth neural network output for input x_k, and d_{jk} is the jth element of d_k, and finally T_r is an index set of training data. The weight parameters (w) are adjusted during training to result in the minimum error [31].

Table 2 Similarities between biological neural networks and artificial neural networks

Biological neural networks	Artificial neural networks
Stimulus	Input
Receptors	Input layer
Neural net	Processing layer(s)
Neuron	Processing element
Effectors	Output layer
Response	Output and an entry

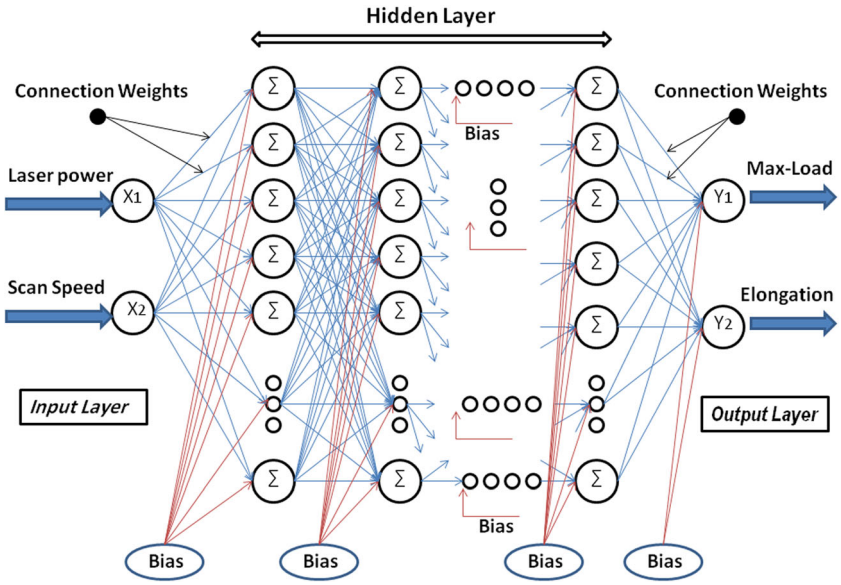

Fig. 3 The applied neural network with five hidden layers

3.2 Neural network setup

Artificial neural networks are networks of highly interconnected neural computing elements that have the ability to respond to input stimuli and to learn and to adapt to the environment. ANN includes two working phases, the phase of learning and recall. In fact, the recall phase works by the weight which obtained from the learning phase based on the input and output dataset [32]. As a nonlinear learning machine, ANNs apply many different processing elements (PEs). Each PE receives connections from other PE and/or itself. Table 2 indicates similarities between biological neural networks and artificial neural networks [33]. There are several empirical methods to investigate and calibrating networks based on mentioned factors. Therefore, using the error processing method can be resulted to find the optimum network.

This research reported a set of different ANNs designed by different learning rules (algorithms) to find the optimum parameters for the laser welding of PET and PET-PEVA polymeric sheets. The empirical parameters contain remarkable effects on the laser welding that is laser power and laser scan speed were used as input processing elements (PEs) in two neural network models. The response maximum amounts of load and elongation were considered as the output. The total samples investigated in both neural networks were divided into three subsamples, which are presented below:

- 70% training
- 15% cross-validation
- 15% testing

Various neural network models applied to find the best solutions for predicting the experimental trends of the laser welding process. The capability and effectiveness of these neural networks were evaluated through two different criteria to make accurate predictions: the root mean square error (RMSE) and the coefficient of correlation (r). The best fit between desired and predicted values would be RMSE = 0 and $r = 1$.

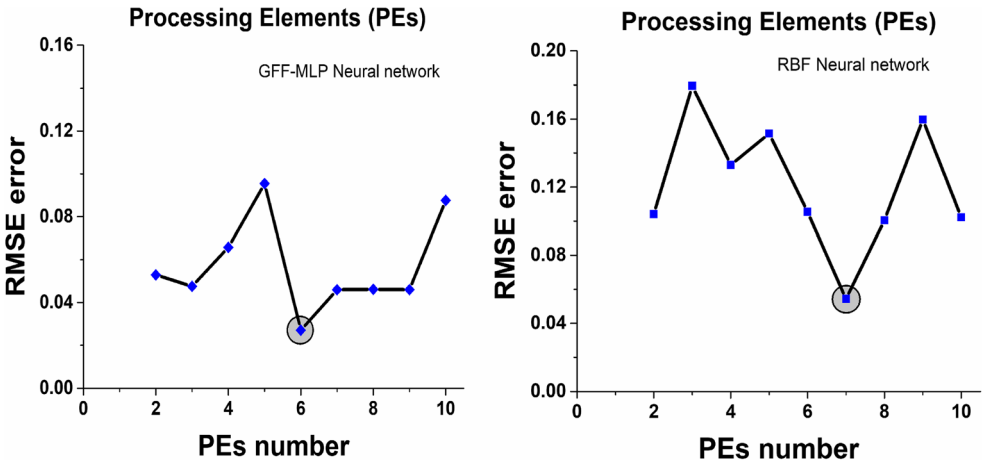

Fig. 4 Analysis of the best PEs number in the hidden layer for the different neural network model

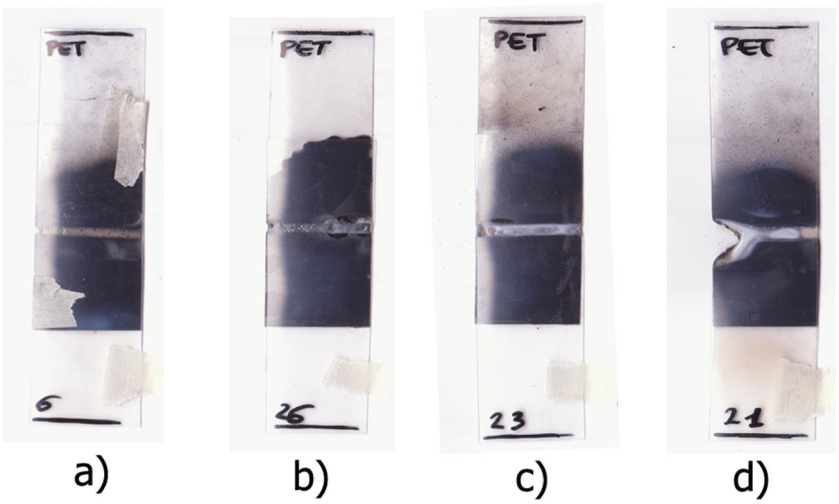

Fig. 5 Four categories of obtained experimental results: **a** no melting, **b** melting-no welded, **c** welded, and **d** welded with degradation

Figure 3 shows the structure of the neural network with five hidden layers which applied to two neural network models. The number of hidden layers is achieved based on the minimum of RMSE number which obtained for five hidden layers. As can be seen, laser power and scan speed were chosen as the input elements, and also max-load and elongation as the output elements. In this study, a Gaussian transfer function was used only in RBF neural network model. Also, the GFF-MLP network applied a sigmoid function as a transfer function for evaluating the accuracy of the predictable tool.

Figure 4 shows the performance of the two neural networks which is applied in this study. The impact of RMSE on the number of PEs in the hidden layer is described. RMSE is minimized when the number of PEs is set at 6 for GFF-MLP neural networks, while RMSE is minimized for RBF neural network when PEs is set at 7. The epoch number for each

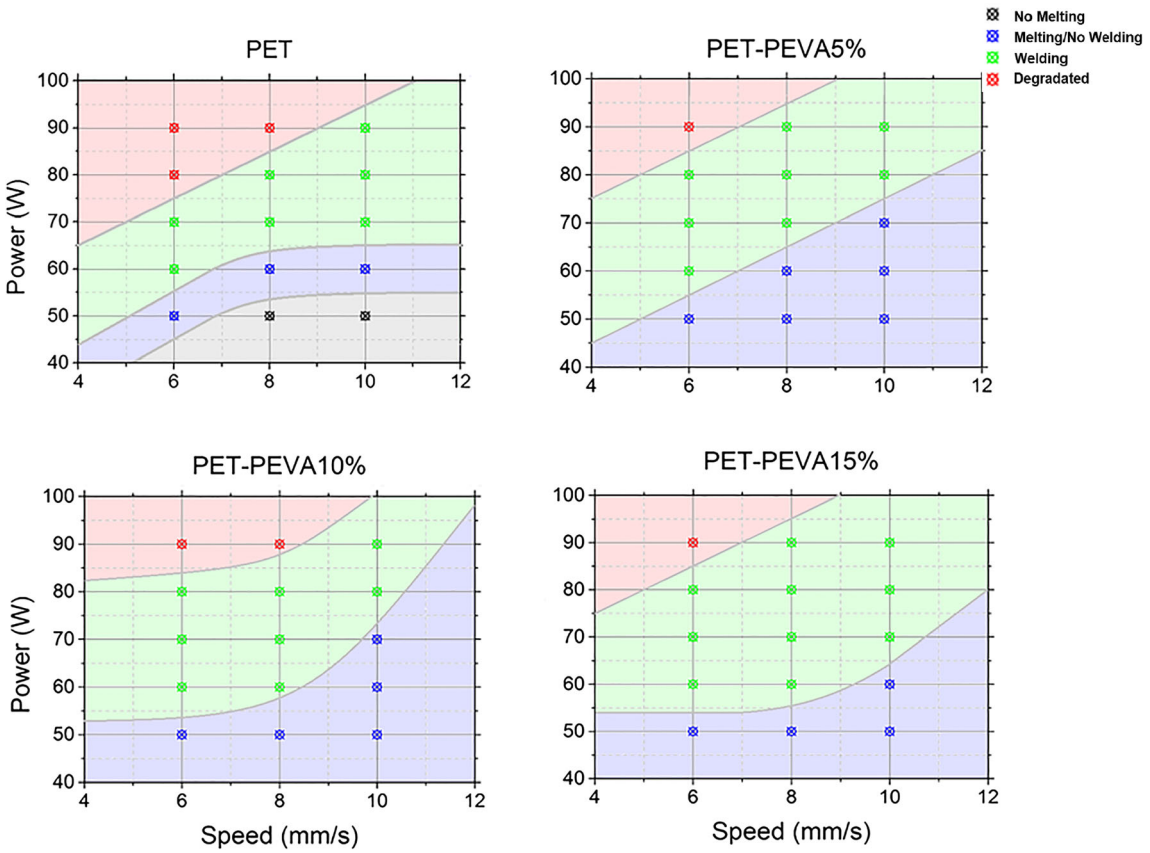

Fig. 6 The visual analysis of the welding process of PET 100% and PET-PEVA 5%, 10%, and 15%

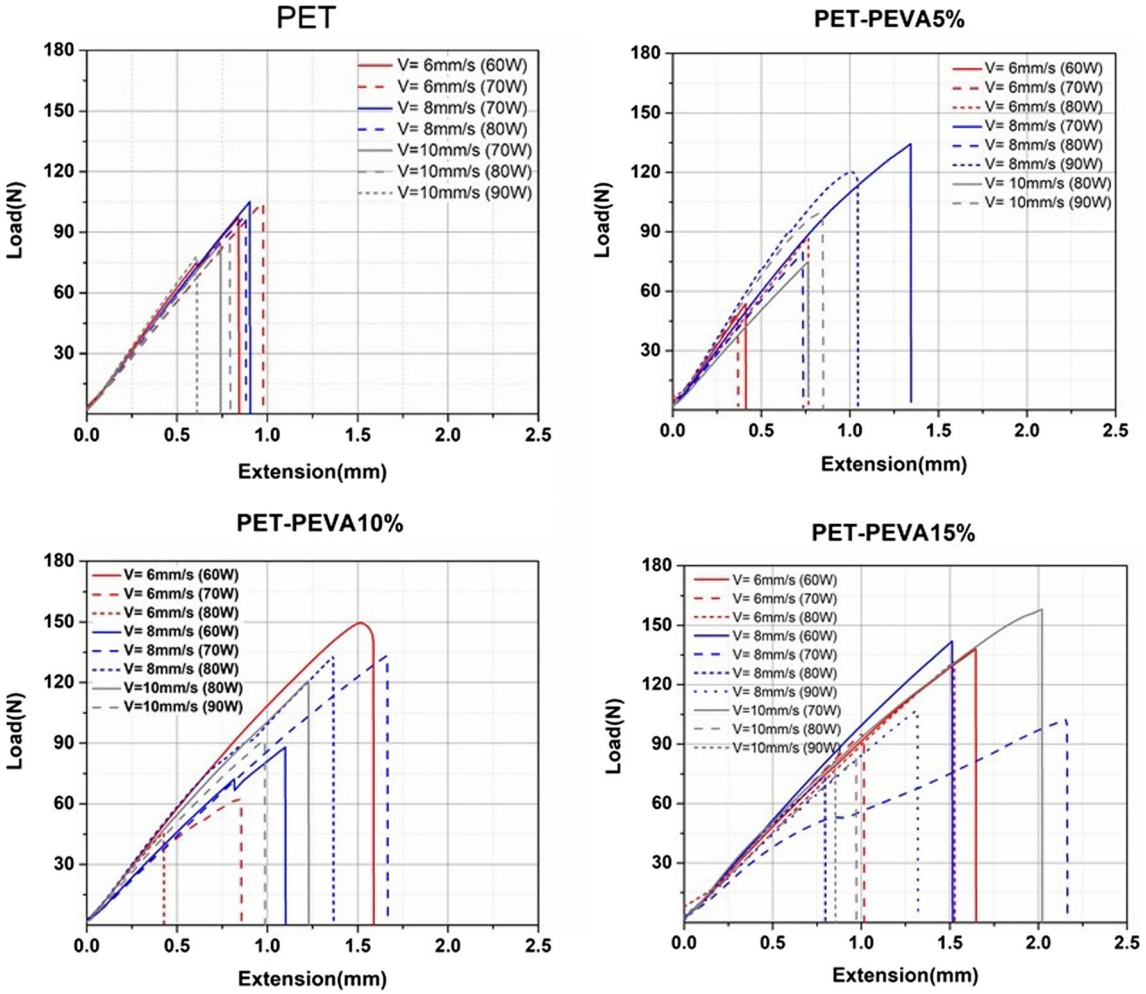

Fig. 7 The results of the mechanical test (load-extension diagram) for all polymeric samples

neural network model was fixed to 1000, except for RBF model in which 1100 epochs, including 1000 epochs for the supervised learning, and 100 epochs for the unsupervised learning.

4 Results and discussion

4.1 The experimental results

Figure 5 shows PET and PET-PEVA samples after the experimental investigation. The samples are classified into four categories: (a) no melting: no melting and adhesion are observed in the faying surface of the polymeric sheets due to the low intensity of the laser radiation; (b) melting/no welded: the forming of welded joint is not stable because of low or mediate laser intensity; (c) welded: the faying surfaces exhibit a sufficient melting and a firm welded joint due to adequate laser intensity; and (d) welded with degradation: the overheating in faying surface resulted in an unacceptable welded joint due to the excess of power density delivered to the plastic surface.

Figure 6 reports a qualitative evaluation of the joints based on the effect of laser operational parameters, including laser power and scan speed, specifically on the weldability of PET 100% and PET-PEVA 5%, 10%, and 15% additive samples. As visible, the green zone of the map represents the ranges of the acceptable parameters for the welding of the polymeric sheets. PET-PEVA 15% boasts a wider range of high-quality welded joints compared to the other polymeric blends since PEVA can absorb more IR wavelength in the overlaying area than the transparent PET during laser irradiation [3, 34].

The mechanical properties of the welded joints were investigated by tensile test through the evaluation of strength and elongation at break. The experimental results showed the samples remained in the elastic range during the tensile tests; then, the breakage of the welded joint suddenly occurred in the interface location where the samples are welded together [35]. Figure 7 shows the results of the tensile test based on various operational parameters, including laser power and scan speed, for all types of polymers. This diagram represents

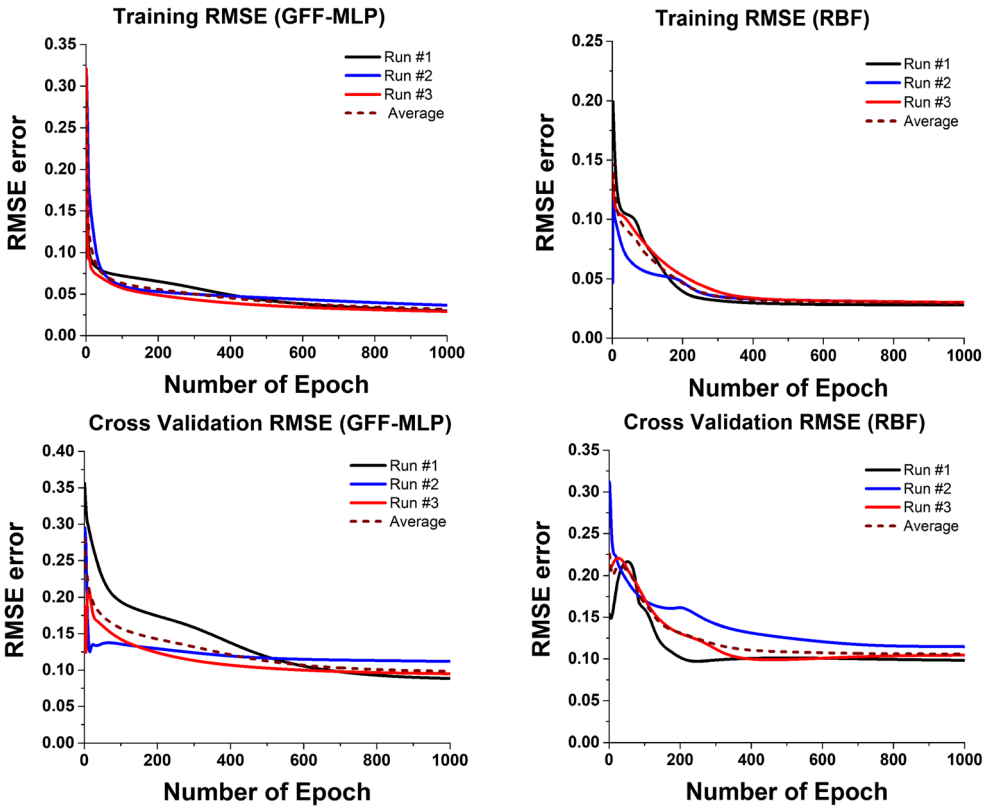

Fig. 8 The trend of RMSE by varying the number of epoch for GFF-MLP (left) and RBF (right) networks

the maximum load and extension for each individual welded sample which was in the green zone of the visual map in Fig. 6. The results are categorized in three different colors based on various laser speeds including 6 mm/s, 8 mm/s, and 10 mm/s.

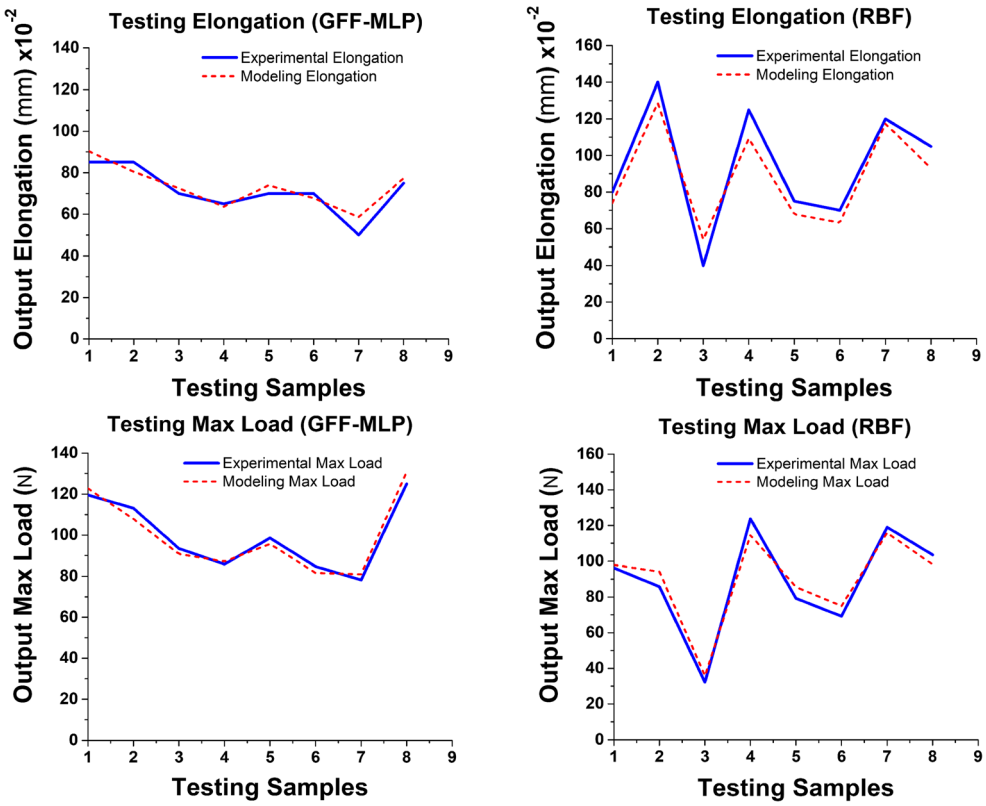

Fig. 9 The trend of RMSE testing elongation (above) and max-load (bottom) by varying the number of epoch for GFF-MLP (left) and RBF (right)

Table 3 Error correction parameters of training and validation for GFF-MLP and RBF networks

All runs	Training minimum	Training standard deviation	Cross-validation minimum	Cross-validation standard deviation
Generalized feed-forward (GFF-MLP)				
Average of final MSEs	0.021824993	0.00414251	0.098351286	0.002091817
Radial basis function (RBF)				
Average of final MSEs	0.039360885	0.001172871	0.10573846	0.008258775

It can be observed that PET-PEVA 15% exhibits the best performance with the maximum strength compared to PET 100%, PET-PEVA 5%, and PET-PEVA 10%, possibly due to the best capability of the opalescent PEVA to absorb the laser radiation in comparison with the nearly transparent pure PET. Therefore, the intrinsic properties of material, like the capability of extension, are modifiable with the addition of PEVA in the PET polymer. Also, the maximum elongations are achieved for PET-PEVA 15% and are significantly higher than other polymers. In fact, the elongation of welded joints significantly increases with the increase in PEVA aliquot inside the blends (PEVA 5%, 10%, and 15%). On average, PET 100% achieved the minimum elongation of 0.97 mm, while PETs blended with PEVA at 5, 10, and 15 wt% show 1.04 mm, 1.09 mm, and 1.10 mm of maximum elongation, respectively. These results confirm how PETs modified with increasing aliquot of PEVA have better strength and elongation (up to 10%) of the welded joints compared to the transparent PET.

4.2 Modeling of experimental data and results

GFF-MLP and RBF neural network models have applied with BP algorithm for modeling the available experimental data, both the strength and the elongation of the different sample investigated. Figure 8 reports the trend of the RMSE according to epoch numbers for both GFF-MLP and RBF networks on the left and right sides. The training was repeated three times to minimize the resulting variability, and the network weights, which minimized the RMSE of the cross-validation, were chosen as the best weights. The best values of process element (PE) were adopted in the hidden layers so that the best topology of the neural networks could be found and 1000 epochs were fixed for each model. As can be seen, the trend of the average values for the training and cross-validation set during the learning process is lower for GFF-MLP model than for the RBF model.

Figure 9 also represents the performance of GFF-MLP and RBF models with reference to the available experimental data (maximum load, bottom, and, elongation, above) for both networks. The trend of the designed networks was displayed according to the number of epochs. GFF-MLP network shows better learning because of lower error compared to the RBF model. In fact, for GFF-MLP, the precision of results during training improved and training time increased.

Standard deviation (SD) represents the variation or dispersion of a data set and can specify the distribution of a dataset compared to the mean value. Table 3 presents the error correction parameters and the results of training and cross-validation for both GFF-MLP and RBF networks based on the comparison of final mean square errors (MSEs). As visible, the achieved results proved that the value of the final MSE is significantly lower for GFF-MLP network than the RBF model. Moreover, Table 4 shows the best network and regression model in accordance with the result of training and cross-validation for GFF-MLP and RBF networks. The number of run, epoch, and regression is the elements compared in these two neural networks. Consequently, GFF-MLP network proved a good capability as a prediction tool, with a fitting of over 98 and 97%, for training and cross-validation values in order, which is higher than those achievable by RBF neural network model.

Table 4 Best network and a regression model for the different neural network with 1000 epochs

Best network model	Training	Cross-validation
Generalized feed-forward (GFF-MLP)		
Run #	3	1
Epoch #	1000	1000
Regression	0.98916114	0.973707277
Radial basis function (RBF)		
Run #	1	1
Epoch #	1000	247
Regression	0.962683697	0.941057339

5 Conclusion

The present study investigated weldability of some polymeric blends, namely PET 100%, PET-PEVA 5%, 10%, and 15% sheets. An appropriate set of operational parameters was found based on the mechanical characterization tests. Accordingly, the following pointwise conclusions can be drawn:

- Thermal sensitivity of PET and PET-PEVA is very close. However, PET-PEVA 15%, despite featuring a large aliquot of a biodegradable polymer, boasts a wider range of weldability if compared with the other blends;
- The influence of PEVA aliquots in PET was found to improve the mechanical properties of the resulting blends in terms of both maximum load and elongation based on the experimental evidence;
- The artificial neural network model was applied as a prediction tool for optimizing the setting of laser parameters, specifically laser power and scan speed. Accordingly, GFF-MLP model was found to be the best neural network solution based on the fitting between measured data and predicted data.
- The simulation results show a very good agreement of the numerical data with the available experimental data for a wide range of operational parameters of the laser welding process.

In conclusion, the establishment of welded joints in PET and PET/PEVA blends by high-power diode laser involves a quick, easy, and low-impact process, easily predictable by neural network modeling. Therefore, welding by high-power diode laser of polymeric blends offers of a viable option in several industrial domains, where easy processing, accurate control, and high level of automation is required.

References

1. Speka M, Matteï S, Pilloz M, Ilie M (2008) The infrared thermography control of the laser welding of amorphous polymers. NDT&E Int 41:178–183
2. Zak G, Mayboudi L, Chen M, Bates PJ, Birk M (2010) Weld line transverse energy density distribution measurement in laser transmission welding of thermoplastics. J Mater Process Technol 210: 24–31
3. Gisario A, Veniali F, Barletta M, Tagliaferri V, Vesco S (2017) Laser transmission welding of poly (ethylene terephthalate) and biodegradable poly (ethylene terephthalate)–based blends. Opt Lasers Eng 90:110–118
4. Brown N, Kerr D, Jackson M, Parkin R (2000) Laser welding of thin polymer films to container substrates for aseptic packaging. Opt Laser Technol 32:139–146
5. Gisario A, Mehrpouya M, Pizzi E (2017) Dissimilar joining of transparent poly (ethylene terephthalate) to aluminum 7075 sheets using a diode laser. J Laser Appl 29:022418
6. Coelho J, Abreu M, Pires M (2000) High-speed laser welding of plastic films. Opt Lasers Eng 34:385–395
7. Mehrpouya M, Lavvafi H, and Darafsheh A (2018) "Microstructural characterization and mechanical reliability of laser-machined structures," in Advances in laser materials processing (second Edition), ed: Elsevier, pp. 731–761
8. Gisario A, Barletta M, Venettacci S, Veniali F (2015) External force-assisted LaserOrigami (LO) bending: shaping of 3D cubes and edge design of stainless steel chairs. J Manuf Process 18: 159–166
9. Gisario A, Mehrpouya M, Venettacci S, Barletta M (2017) Laser-assisted bending of titanium Grade-2 sheets: experimental analysis and numerical simulation. Opt Lasers Eng 92:110–119
10. von Bülow JF, Bager K, Thirstrup C (2009) Utilization of light scattering in transmission laser welding of medical devices. Appl Surf Sci 256:900–908
11. Geiger M, Frick T, Schmidt M (2009) Optical properties of plastics and their role for the modelling of the laser transmission welding process. Prod Eng 3:49–55
12. Mayboudi L, Birk A, Zak G, and Bates P (2006) "Thermal imaging studies and 3-D thermal finite element modeling of laser transmission welding of a lap-joint," in ASME 2006 international mechanical engineering congress and exposition, pp. 423–432
13. Mehrpouya M, Gisario A, Brotzu A, Natali S (2018) Laser welding of NiTi shape memory sheets using a diode laser. Opt Laser Technol 108C:142–149
14. Ilie M, Cicala E, Grevey D, Mattei S, Stoica V (2009) Diode laser welding of ABS: experiments and process modeling. Opt Laser Technol 41:608–614
15. Ilie M, Kneip J-C, Matteï S, Nichici A, Roze C, Girasole T (2007) Through-transmission laser welding of polymers–temperature field modeling and infrared investigation. Infrared Phys Technol 51:73–79
16. Ussing T, Petersen L, Nielsen C, Helbo B, Højslet L (2007) Micro laser welding of polymer microstructures using low power laser diodes. Int J Adv Manuf Technol 33:198–205
17. Amanat N, Chaminade C, Grace J, McKenzie DR, James NL (2010) Transmission laser welding of amorphous and semi-crystalline poly-ether–ether–ketone for applications in the medical device industry. Mater Des 31:4823–4830
18. Chen M, Zak G, Bates PJ (2011) Effect of carbon black on light transmission in laser welding of thermoplastics. J Mater Process Technol 211:43–47
19. Sterjovski Z, Nolan D, Carpenter K, Dunne D, Norrish J (2005) Artificial neural networks for modelling the mechanical properties of steels in various applications. J Mater Process Technol 170:536–544
20. LM L, ML Z, JT N, ZD Z (2001) Predicting effects of diffusion welding parameters on welded joint properties by artificial neural network. Trans Nonferrous Metals Soc China (Eng Ed) 11:475–478
21. Jeng J-Y, Mau T-F, Leu S-M (2000) Prediction of laser butt joint welding parameters using back propagation and learning vector quantization networks. J Mater Process Technol 99:207–218
22. Acherjee B, Mondal S, Tudu B, Misra D (2011) Application of artificial neural network for predicting weld quality in laser transmission welding of thermoplastics. Appl Soft Comput 11:2548–2555
23. Wang X, Zhang C, Li P, Wang K, Hu Y, Zhang P, Liu H (2012) Modeling and optimization of joint quality for laser transmission joint of thermoplastic using an artificial neural network and a genetic algorithm. Opt Lasers Eng 50:1522–1532
24. Naumetc D (2017) "Building the artificial neural network environment: artificial neural networks in plane control,"
25. Karlik B, Olgac AV (2011) Performance analysis of various activation functions in generalized MLP architectures of neural networks. Int J Artif Intell Expert Syst 1:111–122
26. Lipton ZC, Berkowitz J, and Elkan C (2015) "A critical review of recurrent neural networks for sequence learning," arXiv preprint arXiv:1506.00019
27. Broomhead DS and Lowe D (1988) "Radial basis functions, multivariable functional interpolation and adaptive networks," Royal Signals and Radar Establishment Malvern (United Kingdom)

28. Aguilar DP (2004) "A radial basis neural network for the analysis of transportation data,"
29. Rumelhart DE, Hinton GE, Williams RJ (1986) Learning representations by back-propagating errors. nature 323:533–536
30. Schmidhuber J (2015) Deep learning in neural networks: an overview. Neural Netw 61:85–117
31. Burrascano P, Fiori S, Mongiardo M (1999) A review of artificial neural networks applications in microwave computer-aided design (invited article). Int J RF Microwave Comput Aided Eng 9:158–174
32. Mirjalili S, Mirjalili SM, Lewis A (2014) Let a biogeography-based optimizer train your multi-layer perceptron. Inf Sci 269:188–209
33. Guresen E, Kayakutlu G (2011) Definition of artificial neural networks with comparison to other networks. Procedia Comput Sci 3: 426–433
34. Grewell D, Benatar A (2007) Welding of plastics: fundamentals and new developments. Int Polym Process 22:43–60
35. Kang M, Jeon I-H, Han HN, Kim C (2018) Tensile–shear fracture behavior prediction of high-strength steel laser overlap welds. Metals 8:365